

Charm Baryon Studies at BaBar

by V.Ziegler on behalf of the BaBar collaboration

11th International Conference on Hadron Spectroscopy (Hadron05),
08/21/2005--8/26/2005, Rio de Janeiro, Brazil

Stanford Linear Accelerator Center, Stanford University, Stanford, CA 94309

Work supported by Department of Energy contract DE-AC02-76SF00515.

Charm Baryon Studies at *BABAR*

Veronique Ziegler (On behalf of the *BABAR* Collaboration)

Dept. of Physics and Astronomy, University of Iowa, 203 VAN, Iowa City, IA 52242, USA

Abstract. We present a precision measurement of the mass of the Λ_c^+ and studies of the production and decay of the Ω_c^0 and Ξ_c^0 charm baryons using data collected by the *BABAR* experiment. To keep the systematic uncertainty as low as possible, the Λ_c^+ mass measurement is performed using the low Q-value decays, $\Lambda_c^+ \rightarrow \Lambda^0 K_S^0 K^+$ and $\Lambda_c^+ \rightarrow \Sigma^0 K_S^0 K^+$. Several hadronic final states involving an Ω^- and a Ξ^- hyperon are analyzed to reconstruct the Ξ_c^0 and the Ω_c^0 .

Keywords: Charm baryons

PACS: 13.30.Eg, 14.20.Lq

INTRODUCTION

High luminosity colliders and flavor factories provide excellent opportunities to study the properties of charm baryons with high precision. Using the large charm hadron samples available at *BABAR* the Λ_c^+ mass is measured with a precision significantly improved over the existing PDG value[1]. In addition, a study of the production (from $e^+e^- \rightarrow c\bar{c}$ and from B decays) of the Ξ_c^0 charmed baryon and of its decay into $\Omega^- K^+$ and $\Xi^- \pi^+$ is carried out, and a measurement, also improved in precision over previous results[2], for the ratio the branching fractions $\mathcal{B}(\Xi_c^0 \rightarrow \Omega^- K^+)/\mathcal{B}(\Xi_c^0 \rightarrow \Xi^- \pi^+)$ is obtained. Similarly, the decay of the Ω_c^0 baryon reconstructed into: $\Omega_c^0 \rightarrow \Omega^- \pi^+$, $\Omega_c^0 \rightarrow \Xi^- K^- \pi^+ \pi^+$, and $\Omega_c^0 \rightarrow \Omega^- \pi^- \pi^+ \pi^+$ is investigated and the ratios of branching fractions relative to the $\Omega^- \pi^+$ decay mode are measured. A first clear evidence for Ω_c^0 production from B decays is shown. Charge conjugate reactions are implied throughout. The *BABAR* detector is described elsewhere[3].

MEASUREMENT OF THE Λ_c^+ MASS

Since systematic uncertainties related to track reconstruction, involving energy-loss correction and magnetic field strength scale with Q-value,¹ the Λ_c^+ is reconstructed into its low Q-value final states $\Lambda_c^+ \rightarrow \Lambda^0 K_S^0 \pi^+$, $\Lambda^0 \rightarrow p\pi^-$, $K_S^0 \rightarrow \pi^+\pi^-$ (Q= 178 MeV/c²) and $\Lambda_c^+ \rightarrow \Lambda^0 K_S^0 \pi^+$, $\Sigma^0 \rightarrow p\pi^-$, $K_S^0 \rightarrow \pi^+\pi^-$ (Q= 101 MeV/c²), for which the systematic uncertainties in the mass measurement are considerably smaller compared to dominant high Q-value modes such as $\Lambda_c^+ \rightarrow pK^- \pi^+$. The large Q-value modes are used as control samples to study systematic uncertainties. This measurement was done on 232 fb⁻¹ of *BABAR* data.

¹ The Q-value for the decay $a \rightarrow b + c + \dots$ is defined as $Q = m(a) + m(b) + m(c)$

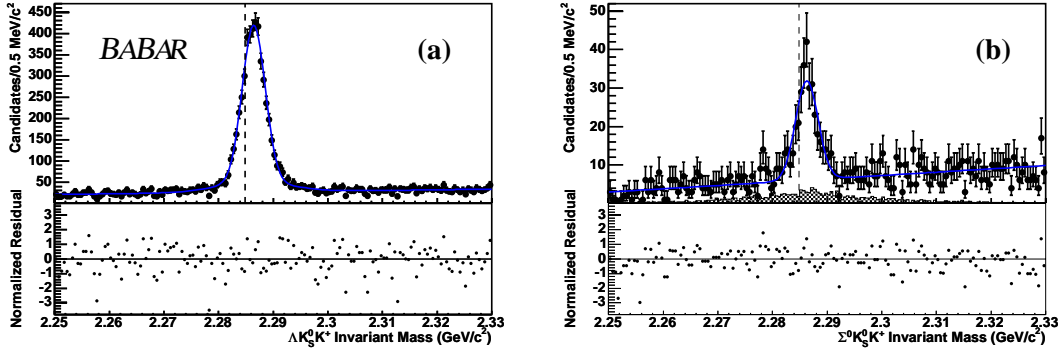


FIGURE 1. Invariant mass distributions for reconstructed Λ_c^+ candidates, for (a) $\Lambda^0 K_S^0 K^+$, and (b) $\Sigma^0 K_S^0 K^+$. The dashed line indicates the present PDG value.

Since the hyperons and the K_S^0 are long-lived particles, the signal-to-background ratio is improved by requiring that their decay vertexes be clearly displaced from that of the parent particle. Particle ID selectors for the proton and the kaon, based on dE/dx measurements given by the Silicon Vertex Tracker (SVT) and the Drift Chamber as well as Cherenkov angle information, have been employed. Only intermediate states with an invariant mass within 3σ of the central PDG value are selected.² The invariant mass is then constrained to the nominal value. These criteria are also required in the selection of the other charm baryons described in this letter. In addition, to reduce combinatorial background coming mostly from B decays, the momentum of the Λ_c^+ candidate in the e^+e^- center-of-mass frame (p^*) is required to exceed 2 GeV/c. Clear Λ_c^+ signal peaks for both modes are shown in Figures 1 (a) and (b). The presence of a peaking background (absorbed into the signal and background) in $\Lambda_c^+ \rightarrow \Sigma^0 K_S^0 K^+$ is due a wrong photon vertexed with a real Λ^0 in the candidate selection. The main systematic uncertainty on the Λ_c^+ mass arises from the energy-loss corrections in charged particle tracking; it is studied using the uncorrected invariant-mass distributions of control samples $\Lambda^0 \rightarrow p\pi^-$ and $K_S^0 \rightarrow \pi^+\pi^-$. The long lifetimes of these hadrons enable us to study their fitted mass values as a function of the their radial decay distance from the interaction point. Figure 2 shows that the largest K_S^0 fitted mass deviations from the PDG mean occur at low decay radii, indicating the under-estimation of the amount of detector material assumed in the track reconstruction algorithm. The effect of increasing the SVT density assumed in the track reconstruction algorithm by 20% removes the radial dependence of the K_S^0 fitted mass. The dips seen in the distribution are reconstruction artifacts also seen in the reconstruction of simulated data. Another way to investigate the the energy-loss correction is to study the fitted mass as a function of the particle momentum using the high Q-value Λ_c^+ control samples. Similarly, increasing the density of the SVT by 20% removes the momentum dependence of the Λ_c^+ fitted mass. The other major sources of systematic uncertainties are the magnetization of the *BABAR* PEP II

² σ corresponds to the invariant mass resolution.

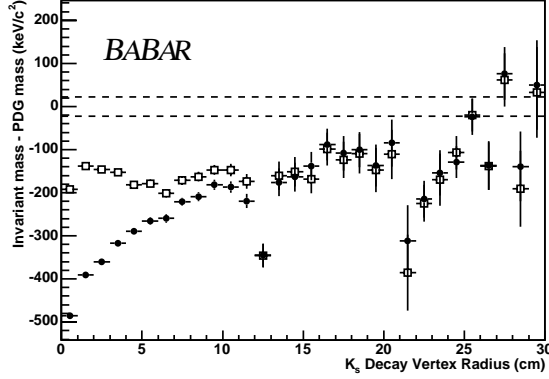


FIGURE 2. The fitted mass values for $K_S^0 \rightarrow \pi^+ \pi^-$ candidates minus the PDG value as a function of the decay radius. The solid circles are for track reconstruction with the normal amount of detector material. The open squares are for track reconstruction assuming 20% more material in the SVT. The dashed lines show the $\pm 1\sigma$ uncertainty on the PDG value for the masses.

permanent magnets³ by the solenoidal field and the dependence of the fitted mass value on the azimuthal angle ϕ of the hadron candidate momentum at the origin. The low Q-value fitted Λ_c^+ mass values are corrected for the under-estimated energy loss by increasing the material density of the SVT by 20%, and the systematic uncertainties in these modes are determined using the dominant high Q-value modes.

Taking into account the energy-loss corrections and correlated systematic uncertainties, we obtain a combined mass measurement for the two low Q-value modes: $m(\Lambda_c^+) = 2286.46 \pm 0.14 \text{ MeV}/c^2$.

PRODUCTION AND DECAY OF THE Ξ_c^0 BARYON

The production and decay of the Ξ_c^0 baryon is studied using 116 fb^{-1} of *BABAR* data. The intermediate states are reconstructed through the decays: $\Xi^- \rightarrow \Lambda \pi^-$, $\Omega^- \rightarrow \Lambda K^-$. To measure the ratio of branching fractions, the requirement that $p^* > 1.8 \text{ GeV}/c$ is imposed on the Ξ_c^0 candidates improving the signal purity. Furthermore, in order to select a region of high and uniform reconstruction efficiency, the polar angle of the Ξ_c^0 candidate with respect to the collision axis in the center-of-mass frame (θ^*) is limited to the range $-0.8 \leq \cos \theta^* \leq 0.8$ for the $\Xi^- \pi^+$ mode and $-0.8 \leq \cos \theta^* \leq 0.6$ for $\Omega^- K^+$. Taking the ratio of the efficiency-corrected yields for each mode, we obtain:

$$\frac{\mathcal{B}(\Xi_c^0 \rightarrow \Omega^- K^+)}{\mathcal{B}(\Xi_c^0 \rightarrow \Xi^- \pi^+)} = 0.294 \pm 0.018(\text{stat.}) \pm 0.016(\text{syst.}),$$

where the dominant systematic uncertainty comes from fits to the mass spectra.

The p^* spectrum of the Ξ_c^0 baryons (allowing for $p^* \leq 1.8 \text{ GeV}/c$) gives an insight into the production mechanisms of $c\bar{c}$ and $B\bar{B}$ events. Figure 3 (d) shows the background-

³ made of Samarium Cobalt (permeability $\mu \approx 1.13$)

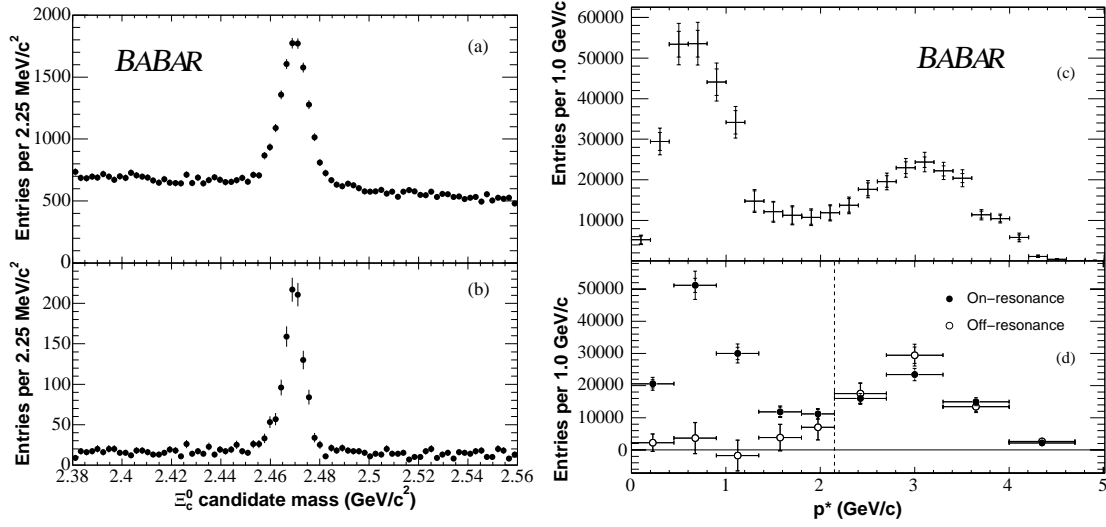


FIGURE 3. Left-hand side: Invariant mass distributions for Ξ_c^0 candidates in data for (a) $\Xi^- \pi^+$, and (b) $\Omega^- K^+$. Right-hand side: The p^* spectrum of Ξ_c^0 candidates decaying via $\Xi^- \pi^+$ shown for the on-resonance data sample (c), and for the on-resonance and off-resonance data samples together (d). The vertical line at 2.15 GeV/c shows the kinematic cutoff for Ξ_c^0 production in B decays at BABAR. The inner error bars give the statistical uncertainty and the outer error bars give the sum in quadrature of the statistical and systematic uncertainties.

subtracted, efficiency-corrected p^* distribution for $\Xi_c^0 \rightarrow \Xi^- \pi^+$ simultaneously for the off-resonance (collected at approximately 40 MeV/c² below the $B\bar{B}$ production threshold), corresponding to Ξ_c^0 production from $e^+e^- \rightarrow c\bar{c}$ only, and for the on-resonance (at the $B\bar{B}$ production threshold) data. The absence of a low p^* peak in off-resonance data substantiates the assumption that the low p^* peak observed in the on-resonance data sample distribution originates from Ξ_c^0 produced from B decays. A similar behavior is seen for the $\Omega^- K^+$ decay mode. Comparing the on-resonance and scaled off-resonance samples for $p^* \leq 2.15$ GeV/c gives the yield of Ξ_c^0 produced in B decays and a value:

$$\mathcal{B}(B \rightarrow \Xi_c^0 X) \times \mathcal{B}(\Xi_c^0 \rightarrow \Xi^- \pi^+) = (2.11 \pm 0.19(stat.) \pm 0.25(syst.)) \times 10^{-4}.$$

The cross section from $e^+e^- \rightarrow c\bar{c}$ is obtained from the yield of Ξ_c^0 produced in $c\bar{c}$ events using the scaled off-resonance data set (for $p^* \leq 2.15$ GeV/c) and the on-resonance data set (for $p^* > 2.15$ GeV/c).

$$\sigma(e^+e^- \rightarrow \Xi_c^0 X) \times \mathcal{B}(\Xi_c^0 \rightarrow \Xi^- \pi^+) = (388 \pm 39(stat.) \pm 41(syst.)) \text{ fb}.$$

PRODUCTION AND DECAY OF THE Ω_c^0 BARYON

The Ω_c^0 charmed baryon is reconstructed into its $\Omega^- \pi^+$ and $\Omega^- \pi^- \pi^+ \pi^+$ final states using 225 fb⁻¹ of BABAR data. And the data sample used to reconstruct $\Omega_c^0 \rightarrow \Xi^- K^- \pi^+ \pi^+$

BABAR
preliminary

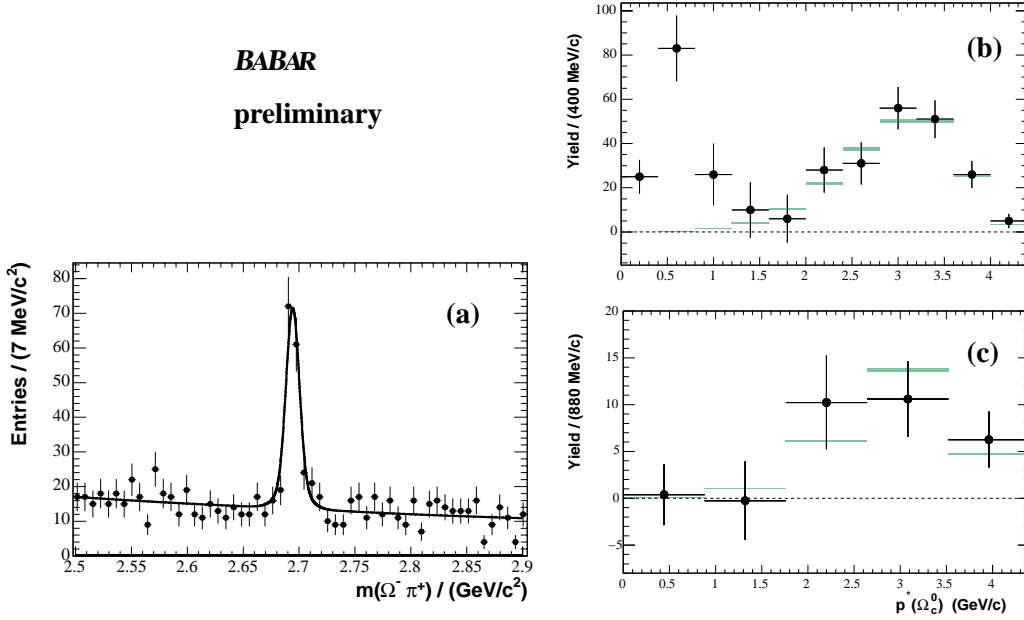


FIGURE 4. Left-hand side: Invariant mass distribution for reconstructed $\Omega_c^0 \rightarrow \Omega^- \pi^+$ shown in (a). Right-hand side: The p^* spectrum of Ω_c^0 candidates decaying via $\Omega^- \pi^+$ shown for the on and off-resonance data samples together in (b), and separately for the off-resonance data sample only in (c). The dots correspond to the data (statistical error bars only) and the solid horizontal bar indicate the predictions for the p^* distribution of Ω_c^0 baryons produced from $e^+e^- \rightarrow c\bar{c}$.

corresponds to an integrated luminosity of 230 fb^{-1} . High values of p^* are necessary to suppress combinatorial backgrounds in the multi-body Ω_c^0 decays; a common minimum p^* of $2.8 \text{ GeV}/c$ is required for candidates used in the measurement of ratios of branching fractions. Figure 4 (a) shows the reconstructed invariant mass spectrum for $\Omega_c^0 \rightarrow \Omega^- \pi^+$. A clear peak is observed. Taking the ratio of the efficiency-corrected yields for Ω_c^0 signal events, extracted from the invariant mass spectra, we obtain a value for the ratio of branching fractions:

$$\frac{\mathcal{B}(\Omega_c^0 \rightarrow \Xi^- K^- \pi^+ \pi^+)}{\mathcal{B}(\Omega_c^0 \rightarrow \Omega^- \pi^+)} = 0.31 \pm 0.15(\text{stat.}) \pm 0.04(\text{syst.}).$$

Since no significant excess of signal events over the background is observed in the $\Omega_c^0 \rightarrow \Omega^- \pi^- \pi^+ \pi^+$ mode, we calculate a limit at the 90% confidence level (CL) on the ratio of branching fractions.

$$\frac{\mathcal{B}(\Omega_c^0 \rightarrow \Omega^- \pi^- \pi^+ \pi^+)}{\mathcal{B}(\Omega_c^0 \rightarrow \Omega^- \pi^+)} \leq 0.3(90\% \text{CL})$$

Figure 4 (b) and (c) show the uncorrected p^* distribution of Ω_c^0 candidates for the entire data sample and the off-resonance only sample, respectively; clear evidence of Ω_c^0 production from B decays is visible at low p^* and is absent in the off-resonance data, collected below the $B\bar{B}$ production threshold.

SUMMARY

We have presented a precision measurement of the Λ_c^+ mass $m(\Lambda_c^+) = 2286.46 \pm 0.14 \text{ MeV}/c^2$, using the low Q-value modes $\Lambda_c^+ \rightarrow \Lambda^0 K_S^0 K^+$ and $\Lambda_c^+ \rightarrow \Sigma^0 K_S^0 K^+$.

We have measured the ratio of branching fractions

$$\frac{\mathcal{B}(\Xi_c^0 \rightarrow \Omega^- K^+)}{\mathcal{B}(\Xi_c^0 \rightarrow \Xi^- \pi^+)} = 0.294 \pm 0.018(\text{stat.}) \pm 0.016(\text{syst.}),$$

and studied the production of Ξ_c^0 from $e^+e^- \rightarrow c\bar{c}$ and measured:

$$\sigma(e^+e^- \rightarrow \Xi_c^0 X) \times \mathcal{B}(\Xi_c^0 \rightarrow \Xi^- \pi^+) = (388 \pm 39 \pm 41) \text{ fb.}$$

We have presented an observation of the production of Ξ_c^0 from B decays:

$$\mathcal{B}(B \rightarrow \Xi_c^0 X) \times \mathcal{B}(\Xi_c^0 \rightarrow \Xi^- \pi^+) = (2.11 \pm 0.19(\text{stat.}) \pm 0.25(\text{syst.})) \times 10^{-4}.$$

We obtained a measurement of the ratio of branching fractions

$$\frac{\mathcal{B}(\Omega_c^0 \rightarrow \Xi^- K^- \pi^+ \pi^+)}{\mathcal{B}(\Omega_c^0 \rightarrow \Omega^- \pi^+)} = 0.31 \pm 0.15(\text{stat.}) \pm 0.04(\text{syst.}),$$

and an upper limit for

$$\frac{\mathcal{B}(\Omega_c^0 \rightarrow \Omega^- \pi^- \pi^+ \pi^+)}{\mathcal{B}(\Omega_c^0 \rightarrow \Omega^- \pi^+)} \leq 0.3(90\% \text{CL}).$$

And we have shown a first observation of the decay $B \rightarrow X \Omega_c^0 \rightarrow \Omega^- \pi^+$.

ACKNOWLEDGMENTS

We are grateful for the excellent luminosity and machine conditions provided by our PEP-II colleagues, and for the substantial dedicated effort from the computing organizations that support *BABAR*.

REFERENCES

1. Particle Data Group, S. Eidelman *et al.*, Phys. Lett. B **592**, 1 (2004).
2. CLEO Collaboration, S. Henderson *et al.*, Phys. Lett. B **283**, 161 (1992).
3. The *BABAR* Collaboration, B. Aubert *et al.*, Nucl. Instrum. Methods A **479**, 1 (2002).
4. D. Brown, E. Charles, and D. Roberts, "The *BABAR* Track Fitting Algorithm", contributed paper to CHEP 2000.
5. The *BABAR* Collaboration, B. Aubert *et al.*, hep-ex/0507009, contributed paper to LP 2005.
6. The *BABAR* Collaboration, B. Aubert *et al.*, Phys. Rev. Lett. **95**, 142003 (2005).
7. CLEO Collaboration, B. Barish *et al.*, Phys. Rev. Lett. **79**, 3599 (1997).
8. The *BABAR* Collaboration, B. Aubert *et al.*, hep-ex/0507011, contributed paper to LP 2005.
9. P. L. Frabetti *et al.* [E687 Collaboration], Phys. Lett. B **300**, 190 (1993).
10. P. L. Frabetti *et al.* [E687 Collaboration], Phys. Lett. B **338**, 106 (1994).
11. S. Ahmed *et al.* [CLEO Collaboration], Int. J. Mod. Phys. A **16S1B**, 505 (2001).